Microchim Acta (2017) 184:147–153
DOI 10.1007/s00604-016-1996-z

ORIGINAL PAPER

An ultrasensitive amperometric immunosensor for zearalenones based on oriented antibody immobilization on a glassy carbon electrode modified with MWCNTs and AuPt nanoparticles

Na Liu[1] · Dongxia Nie[2] · Yanglan Tan[1] · Zhiyong Zhao[2] · Yucai Liao[3] · Hui Wang[1] · Changpo Sun[4] · Aibo Wu[1]

Received: 16 May 2016 / Accepted: 21 October 2016 / Published online: 8 November 2016

Abstract The family of zearalenones (ZENs) represents a major group of mycotoxins with estrogenic activity. They are produced by *Fusarium* fungi and cause adverse effects on human health and animal production. The authors describe here a label-free amperometric immunosensor for the direct determination of ZENs. A glassy carbon electrode (GCE) was first modified with polyethyleneimine-functionalized multi-walled carbon nanotubes. Next, gold and platinum nanoparticles (AuPt-NPs) were electro-deposited. This process strongly increased the surface area for capturing a large amount of antibodies and enhanced the electrochemical performance. In a final step, monoclonal antibody against zearalenone was orientedly immobilized on the electrode, this followed by surface blocking with BSA. The resulting biosensor was applied to the voltammetry determination of ZENs, best at a working voltage of 0.18 V (vs SCE). Under optimized conditions, the method displays a wide linear range that extends from 0.005 to 50 ng mL^{-1}, with a limit of detection of 1.5 pg mL^{-1} (at an S/N ratio of 3). The assay is highly reproducible and selective, and therefore provides a sensitive and convenient tool for determination of such mycotoxins.

Keywords Biosensor · Electroanalysis · Mycotoxins · Electrodeposition · Gold nanoparticles · Platinum nanoparticles · Cyclic voltammetry · Differential pulse voltammetry · Food analysis

Introduction

Zearalenones (ZENs), including ZEN and its derivates (α-ZOL, β-ZOL, ZAN, α-ZAL and β-ZAL), are a group of mycotoxins produced by *Fusarium* molds and commonly detected in corn products and other cereal-based foods [1–3]. ZENs may cause reproductive troubles such as less fertility, lower hormone levels and fetal wastage [4, 5]. In order to protect consumers' health, European Union (EU) has set the maximum residue levels (MRLs) for ZEN in foodstuffs, i.e. 350 μg kg^{-1} in unprocessed corn and 20 μg kg^{-1} in both processed corn-based and cereal-based baby foods (Commission Regulation, EC No.1126/2007). Thus, it is urgent to explore sensitive, rapid and simple analytical methods for monitoring the ZENs exposure in foodstuffs concerning human health.

Chromatography methods are commonly used for detecting ZENs because of their high accuracy and reliability [3, 6, 7]. However, these techniques require expensive instruments, as well as sophisiticated pretreatment and clean-up processes for variable matrices in accordance of instrumental

Electronic supplementary material The online version of this article (doi:10.1007/s00604-016-1996-z) contains supplementary material, which is available to authorized users.

✉ Aibo Wu
abwu@sibs.ac.cn

[1] SIBS-UGENT-SJTU Joint Laboratory of Mycotoxin Research, Key Laboratory of Food Safety Research, Institute for Nutritional Sciences, Shanghai Institutes for Biological Sciences, Chinese Academy of Sciences, 294 Taiyuan Road, Shanghai 200031, People's Republic of China

[2] Institute for Agri-food Standards and Testing technology, Shanghai Academy of Agriculture Science, 1000 Jinqi Road, Shanghai 201403, People's Republic of China

[3] College of Plant Science and Technology, Huazhong Agricultural University, No. 1 Shizishan Street, Hongshan District, Wuhan, Hubei 430070, People's Republic of China

[4] Academy of State Administration of Grain, No. 11 Baiwanzhuang Avenue, Xicheng District, Beijing 100037, People's Republic of China

conditions. As an alternative strategy, electrochemical biosensors have gained great interests towards analysis of target biomolecules [8, 9]. With application of monoclonal antibody (MAb), immunoassays have been considered to be a promising approach with high selectivity and sensitivity [10]. Compared with conventional immunosensors with complicated enzyme label, novel label-free immunosensors have been developed for trace analysis, performing direct detection by measuring physical changes of antibody–antigen immunocomplex [11, 12].

Nano-materials have been introduced into a variety of methods for mycotoxin detection [13, 14], especially applied to develop immunosensors for their unique merits. Due to unique structural, mechanical, thermal, and electrical properties, multi-wall carbon nanotubes (MWCNTs) consisting of up to several tens of graphitic shells have been widely applied as one of the most important materials in electrochemical immunosensor [15–18]. Bimetallic nanoparticle is another functional material used in our study and also exploited widely in biochemical analysis. The addition of a second metal brings in particular changes in chemical and physical properties by the interaction between two components, for instance, catalytic activity and chemical selectivity [19, 20]. Gold–platinum alloy nanoparticles (AuPt-NPs) is one of the most useful bimetallic nanoparticle, which has excellent catalysis because of high synergistic action between gold and platinum [21]. By controlling the electrodeposition time and the concentration of metallic nanoparticles solution, the electrodeposition method for metallic nanoparticles immobilization was easily operated and less time-consuming.

The immobilization of antibodies on the electrodes was an important factor in fabricating sensitive immunosensors. Physical adsorption and covalent immobilization of antibodies were usually adopted in immunosensors preparation for the detection of ZEN and its derivates in previous report [22–26]. However, these immobilization methods probably result in the loss of binding capability due to random orientation of the antibodies and significant steric-hindrance [27]. In contrast, oriented immobilization of antibody on the surface of an immunosensor effectively improves biosensor performance [28], which has been achieved adsorption on a sublayer of Fc binding receptors [29]. Staphylococcus proteins A (SPA), derived from the cell wall of *Staphylococcus aureus*, is a bacterial surface protein with four Fc binding domains which specifically bind to the Fc regions of antibody and leave the antigen-binding site free [30–33]. The strategy of SPA-mediated antibody immobilization leads to highly efficient immunoreactions and to a remarkable detection performance [34].

Herein, the aim of this current research work is to explore a label-free electrochemical immunosensor for detecting ZEN and its derivates as family mycotoxins in naturally contaminated matrices. In order to achieve excellent sensitivity, MWCNTs was utilized towards electrode surface to enhance the adsorption capacity due to its large surface area, and AuPt-NPs were deposited to provide a stable surface for SPA immobilization. The oriented immobilization of antibody by modifications with SPA can improve the performance of immunosensor as well. So far, there have been no reports focusing on the detection of a group of mycotoxin by a sensitive label-free immunosensor based on oriented immobilization. In regard to bioanalysis with complicated matrices, this fabricated label-free immunosensor provides a relatively time-saving approach for the detection of family ZENs with wide linear range and low detectable limit.

Experimental

Chemicals

ZENs standards, including zearalenone (ZEN), α-zearalenol (α-ZOL), β-zearalenol (β-ZOL), zearalanone (ZAN), α-zearalanol (α-ZAL), β-zearalanol (β-ZAL), as well as other mycotoxins, ochratoxin A (OTA), aflatoxin B1 (AFB1), and deoxynivalenol (DON) were purchased from Romer Labs, Inc. (Union, MO, USA, http://www.romerlabs.com). $HAuCl_4$ and H_2PtCl_6 were purchased from Sinopharm Chemical Reagent Co. Ltd. (Shanghai, China, http://www.sinoreagent.com). Carboxyl functionalized multiwall carbon nanotubes (MWCNTs) were supplied by Shenzhen Carbon Nanotechnologies Co. Ltd. (Shenzhen, China, http://www.nanotubes.com.cn). Recombinant SPA and staphylococcal protein G (SPG) were brought from Hangzhou Neuropeptide Biological Science and Technology Inc. Ltd. (Hangzhou, China, http://www.NUPTEC.com). MAb used was obtained in our previous work, which was immunized by the ZEN-BSA conjugate and produced via the mouse hybridoma technique [35]. Polyethylenimine (PEI, Mw 25,000) and bovine serum albumin (BSA) were purchased from Sigma-Aldrich (St. Louis, MO, USA, http://www.sigmaaldrich.com). Other chemical reagents were of analytical grade. 0.01 M PBS (pH 7.4) containing 5 mM of $K_3[Fe(CN)_6]/K_4[Fe(CN)_6]$ and 0.1 M KCl was used as working solution.

Apparatus

Cyclic voltammetry (CV) and differential pulse voltammetry (DPV) were performed with a CHI660D electrochemical workstation (Shanghai Chenhua Co., China, http://www.chinstr.com). The conventional three-electrode system was employed with a glassy carbon electrode (GCE, 3.0 mm diameter) as the working electrode, a saturated calomel electrode (SCE) as the reference electrode, and a platinum electrode as the counter electrodes. All electrochemical measurements were carried out at room temperature (25 °C).

Fabrication of the label-free immunosensor

Prior to use, the glassy carbon electrode was polished sequentially with Al_2O_3 powder of 1, 0.3 and 0.05 μm, and cleaned ultra-sonically with distilled water, 6 M nitric acid, absolute ethanol and distilled water for 5 min, respectively. Then, the electrode was immersed in 0.5 M H_2SO_4 for activation under a cycling electrode potential from −1.0 to 1.0 V at a scan rate of 100 mV s^{-1} until stabilization. A detail schematic illustration of the stepwise procedures for immunosensor fabrication was shown in Fig.1.

Synthesis of MWCNT-PEI

The preparation of MWCNT-PEI was conducted by following procedures reported in a previous study with modifications [36]. 1 mg of MWCNTs was dispersed in 1 mL PEI aqueous solution (1 mg mL^{-1}), and the suspension was sonicated for 60 min. 10 μL of MWCNT-PEI solution was dropped on the bare electrode and dried in the air.

Electrodeposition of AuPt-NPs

Electrodeposition of AuPt-NPs was preformed according to a previous research with small modifications [37]. 2 mg mL^{-1} of $HAuCl_4$ and H_2PtCl_6 solution were separately prepared by 0.2 M Na_2SO_4 aqueous solution, and then mixed with a volume ratio of 1:1. Then modified GCE/MWCNT-PEI electrode was immersed into the above mixture solution and electrodeposited at −0.2 V for 30 s to form GCE/MWCNT-PEI/ AuPt-NP electrode.

Antibody-oriented immobilization

A 5 μL of SPA (0.3 μg mL^{-1}) and 5 μL of anti-ZEN MAb (0.1 μg mL^{-1}) were sequentially dropped on the GCE/MWCNT-PEI/AuPt-NP-modified electrode and incubated at 37 °C for 1 h. Unbound SPA and antibodies were washed away with PBS solution after each modification step. Finally, the prepared immunosensor was blocked with 1 % of BSA solution for 1 h at 37 °C to avoid nonspecific adsorption. After carefully washed and dried in air, the electrode was stored at 4 °C prior to analysis.

Mycotoxins detection

For each measurement for ZEN detection, the immunosensor was immersed in the working solution for DPV analysis, generating the peak current as $I_{,BSA}$, followed by incubation in standard or sample solution for 20 min. After the immunosensor was washed carefully with PBS and dried in the air, another measurement of DPV analysis was carried out, recording the peak current as $I_{,ZEN}$. The ZEN detection result was finally based on the current difference of two DPV measurements above ($\Delta I = I_{,BSA} - I_{,ZEN}$).

Results and discussion

Choice of materials

In order to obtain excellent performance, the following materials were carefully selected for sensor construction. MWCNTs were used for supporting nanoparticles and improving electronic conductivity and chemical stability on the electrode because of the unique characteristics to enlarge active surface area. PEI, an amino-rich cationic polyelectrolyte, was chosen as a functional agent, which can interact with MWCNTs via both physisorption and electrostatic adsorption on MWCNTs' sidewalls. AuPt-NPs were selected for depositing on the PEI functionalized MWCNTs for immobilization of SPA, by considering that metallic alloy nanomaterials have better catalytic properties than monometallic counter-parts [38], and Au possesses favorable biocompatibility to protein. On this constructed immunosensor, SPA was adopted for oriented immobilization of antibodies to ensure antibodies

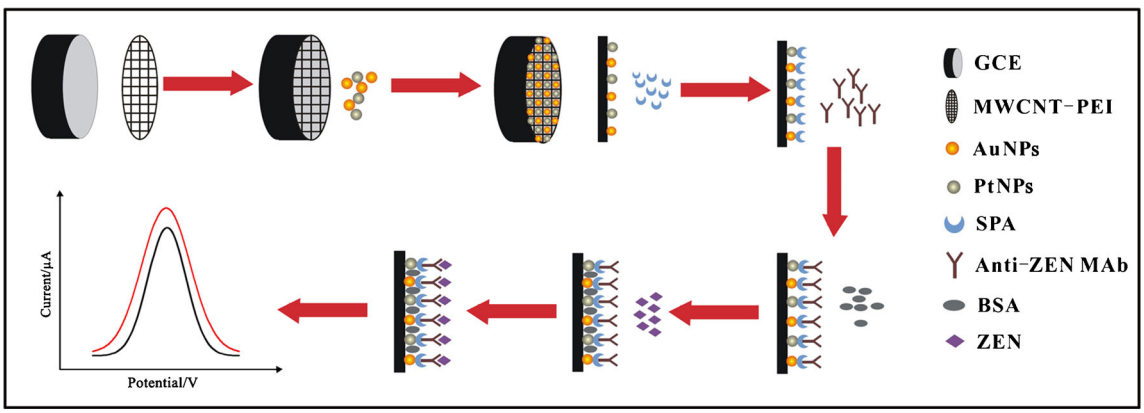

Fig. 1 Schematic illustration of the stepwise immunosensor fabrication process

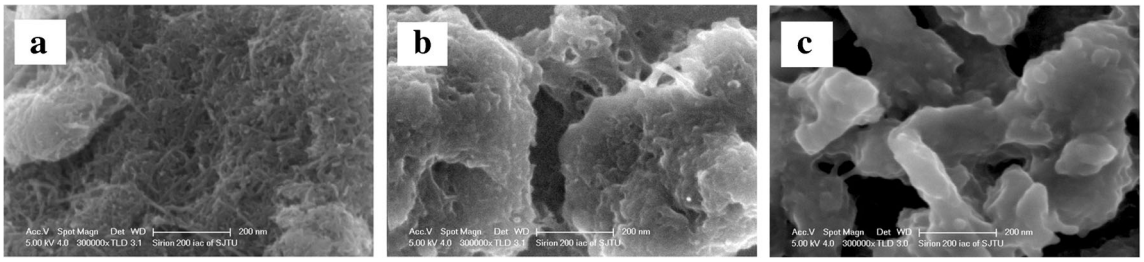

Fig. 2 The SEM identification of the material films used for immunosensor fabrication and immobilized on ITO conducting glass: **a** MWCNT-PEI, **b** MWCNT-PEI/AuPt-NP, **c** MWCNT-PEI/AuPt-NP/SPA

being orientedly anchored on substrate surface through their Fc portion and thus the binding sites of antibodies remaining free and accessible for binding with antigens [33].

Characteristics of the immunosensor

In order to investigate the assembly process of MWCNTs, bimetallic alloys nanoparticles (AuPt-NPs) and SPA films, the morphology of these fabrications was characterized by SEM (Fig. 2). Figure 2a showed that regularly branched MWCNTs were densely embedded and efficiently dispersed within the PEI aqueous solution, which were capable of stabilizing the nanometer-sized metal particles on the external surface. According to Fig. 2b for AuPt-NPs deposition, many anomalous nanoclusters were obtained on the surface of the MWCNTs by means of electrodeposition. The amount of NPs can be controlled by the deposition time, which provided an efficient surface for loading SPA and accelerating the electron transfer. In Fig. 2c, SPA was embedded firmly and uniformly on the surface of metal NPs. This further contributes to oriented immobilization of antibody.

In order to monitor the current changes of the fabricated electrode, the CVs measurements were performed at a scan rate of 100 mV. The CVs of the electrodes at different stages were displayed in Fig. 3a. A reversible $[Fe(CN)^6]^{3-}/[Fe(CN)^6]^{4-}$ redox peaks pair was seen as a curve that corresponds to the bare GCE. After the modification of MWCNT-PEI and following deposition of AuPt-NPs, the amperometric response significantly increased, showing stronger conductivity of the GCE with the modification of MWCNTs and AuPt-NPs (Fig. 3a, curve b and c). However, with the immobilization of SPA and anti-ZEN MAb, the CV response decreased stepwise due to proteins hindering the electrons transfer on the electrode (Fig. 3a, curve d and e). Subsequently, a decline was noticed after the self-assembly of BSA (Fig. 3a, curve f) that blocked possible remaining active sites on the electrode surface. The CV response was further decreased after the fabricated immunosensor was incubated with a 5 ng mL^{-1} ZEN solution prepared in PBS (Fig. 3a, curve g). As shown above, the CV changes were consistent with the conductivity changes upon each experimental step, and verified stepwise assembly of the immunosensor.

Typical CV of the fabricated immunosensor was performed in working solution at different scan rates, shown as Fig.3b (curve a–j). Both the anodic and cathodic peak currents (Ipa and Ipc) were proportional to square root of scan rates in the range from 5 to 400 mV s^{-1}. The regression equations of Ipa and Ipc were listed as follows: Ipa (μA) = −2.8134 + 3.1166 $V^{1/2}$ (mV s^{-1}) (R^2 = 0.9918), Ipc (μA) = 2.6652–3.4536$V^{1/2}$ (mV s^{-1}) (R^2 = 0.9964), indicating that the electrochemical process was a diffusion-controlled reaction (Fig. 3c).

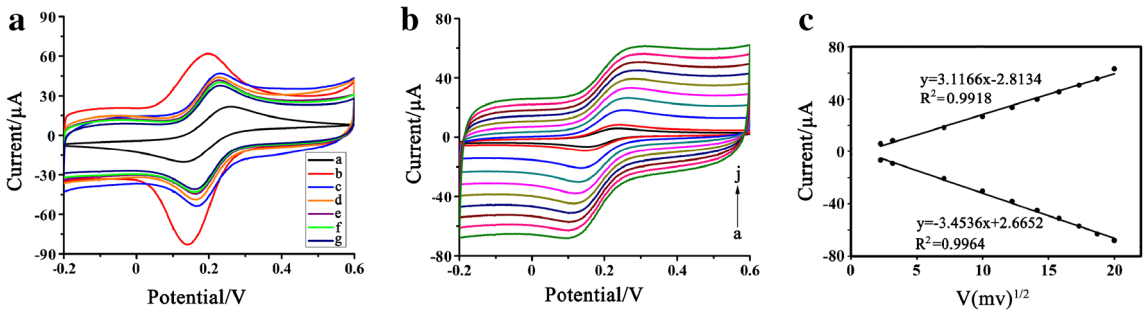

Fig. 3 **a** CVs of modified electrode recorded in the presence of 0.01 M PBS containing 5.0 mM $[Fe(CN)^6]^{3-/4-}$ and 0.1 M KCl, a) bare electrode, b) GCE/MWCNT-PEI electrode, c) GCE/MWCNT-PEI/AuPt-NP electrode, d) GCE/MWCNT-PEI/AuPt-NP/SPA electrode, e) GCE/MWCNT-PEI/AuPt-NP/SPA/MAb electrode, f) GCE/MWCNT-PEI/AuPt-NP/SPA/MAb/BSA electrode, g) GCE/MWCNT-PEI/AuPt-NP/SPA/MAb/BSA/ZEN electrode. **b** CVs of the modified electrodes at different scan rates (from a to j): 5, 10, 50, 100, 150, 200, 250, 300, 350, 400 mV s^{-1} in working buffer. **c** Linear relationship between the anodic peak currents (Ipa, upper) and cathodic peak currents (Ipc, lower) to square root of scan rates

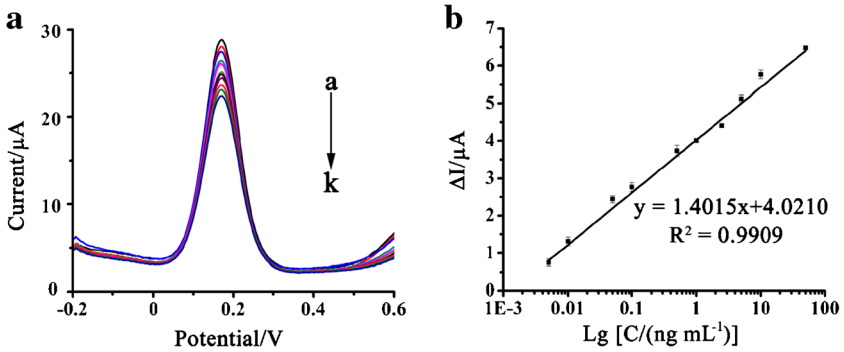

Fig. 4 Calibration plot for ZEN detection obtained with the immunosensor. **a** The DPVs of the immunosensor after incubation in different concentrations of ZEN standard solution (from a to k): 0, 0.005, 0.01, 0.05, 0.1, 0.5, 1, 2.5, 5, 10, and 50 ng mL^{-1}. **b** The linear relationship between the current response at a working potential of 0.18 V (vs SCE) and ZEN concentration in the range of 0.005–50 ng mL^{-1}

Optimization of method

The following parameters were optimized: (a) Metal NPs for electrodeposition; (b) the deposition time of metal NPs; (c) protein for antibody capturing; (d) the concentration and immobilization time of protein for antibody capturing; (e) the concentration and immobilization time of antibody; (f) the pH of working buffer in the detection of ZEN; (g) the incubation time for the detection of ZEN; (h) the blocking time of BSA. Respective data and Figures (Fig. S1 and Fig. S2) are given in the Electronic Supporting Information. The following experimental conditions were found to give best results: (a) AuPt-NPs for electrodeposition; (b) 30 s for deposition of AuPt-NPs; (c) SPA for oriented immobilization of antibodies; (d) 60 min for SPA mobilization at a concentration of 0.3 μg mL^{-1} of SPA solution; (e) 60 min for antibody immobilization with a concentration of 0.1 μg mL^{-1} of antibody solution; (f) the pH of the working solution as 7.4 for ZEN detection; (g) the incubation time of 20 min for ZEN detection; (h) blocking for 60 min with 1 % of BSA solution.

Sensitivity of the immunoassay for ZEN

Under the above optimal conditions, the quantitative range of the ZEN immunosensor was explored. As presented in Fig. 4a, the DPV response decreased with the increase of ZEN concentration. It might be due to antigen-antibody immunocomplex structures formed on the immunosensor which act as electron- transfer barriers [39]. As shown in Fig. 4b, the calibration plots relating the changes of current response (ΔI) was proportional to ZEN concentration over the 0.005–50 ng mL^{-1} range. The linear regression equation is $\Delta I = 4.0210 + 1.4015$ lgC (C: ng mL^{-1}) with $R^2 = 0.9909$. The detection limit (LOD) calculated was 1.5 pg mL^{-1} ($S/N = 3$). The obtained LOD was comparable with the sensitive label-free immunosensor reported previously (1.7 pg mL^{-1}) [21], but the linear range was wider than previous reports listed in Table 1.

Selectivity, stability and reproducibility of the immunosensor

The selectivity of the immunosensor was investigated by comparing the DPV response changes with incubation in ZENs (α-ZOL, β-ZOL, ZAN, α-ZAL and β-ZAL) solution and some other common co-occurring mycotoxins (OTA,DON and AFB1) solution under the same concentration of 50 ng mL^{-1}. Figure 5a showed that the current changes (ΔI) were 6.48 μA for ZEN, 1.6 μA for α-ZAL, 3.74 μA for β-ZAL, 1.39 μA for α-ZOL, 1.73 μA for β-ZOL, and 0.96 μA for ZAN, respectively, while no significant changes were observed for OTA, DON and AFB1 ($\Delta I < 0.15$ μA). The

Table 1 Label-free immunosensors for determination of ZENs

References	Working electrode	Antibody immobilization	Linear range (ng mL^{-1})	LOD (pg mL^{-1})	Target analytes
[23]	GCE/mesoporous carbon@Au-core@AgPt/Ab/BSA	Adsorption	0.005–15	1.7	ZEN
[24]	Gold electrode/graphene sheets-NiNP/Ab/BSA	EDC-NHS	0.05–10	6	Zeranol
[25]	SPCE/MWCNTs-PVP/AuNPs/Ab	EDC-NHS	0.05–50	16	α-zearalanol
[26]	SPCE/Au–PtNPs/Ab	EDC-NHS	0.03–30	10	Zeranol
This study	GCE/MWCNT-PEI/AuPt-NP/SPA/Ab/BSA	SPA orientation	0.005–50	1.5	Family ZENs

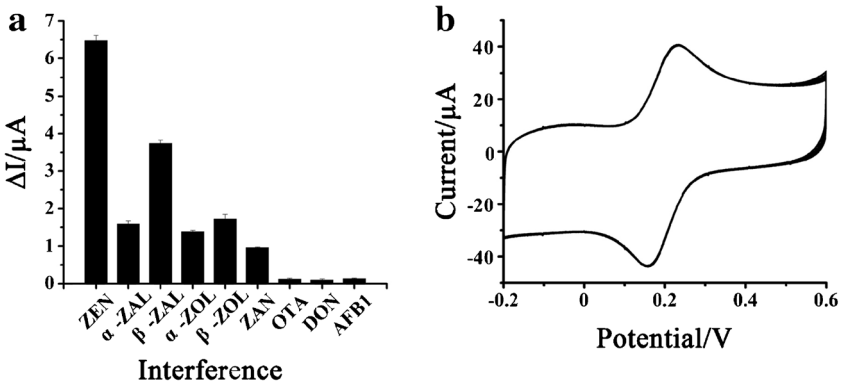

Fig. 5 **a** DPV responses of the prepared immunosensor in nine mycotoxins including family ZENs (ZEN, α-ZAL, β-ZAL, α-ZOL, β-ZOL, and ZAN), OTA, DON, and AFB1. Each mycotoxin solution was prepared in the concentration of 50 ng mL^{-1}. **b** 20-cycle CVs scans of the immunosensor in working buffer

obtained results indicated that the prepared immunosensor detected family ZENs with high selectivity, which was different from previous immunosensors focusing on detection of a single mycotoxin [23–26]. Therefore, the immunosensor can be applied as an indicative tool for ZENs (ZEN, α-ZOL, β-ZOL, ZAN, α-ZAL and β-ZAL) detection without interferences from other mycotoxins.

The reproducibility of the immunosensor was evaluated via testing DPV signals in 0.5 ng mL^{-1} ZEN standard solutions with five prepared immunosensors. Five ΔI values were obtained as 25.82 μA, 25.14 μA, 24.63 μA, 25.98 μA, and 25.32 μA, respectively, with a relative standard deviation (RSD) of 2.13 %. The results validated that the fabricated immunosensor had good reproducibility.

Additionally, by measuring the DPV response in two individual experiments with a 10-day interval, good stability was shown with the result that 89.04 % of its initial signal was retained after 10 days of storage period at 4 °C. Under the optimal conditions, the prepared immunosensor was measured by CVs for a 20-cycle successive scan, and a less than <1 % deviation of initial responds were observed (Fig. 5b).

Performance of the immunoassay

In order to further investigate the performance of the fabricated immunosensors for ZEN analysis in real samples, two types of corn products, including corn flour and corn based baby food were chosen as matrices. As verified by LC-MS/MS, the contamination levels of ZENs were 1.53 μg kg^{-1} in corn flour and 0.31 μg kg^{-1} in corn based baby food respectively. After 5 g of each product was spiked with ZEN standard solution with three spiking levels respectively, the samples were treated with 25 mL of 70 % methanol solution. The ZEN extracting solution was then 5-fold diluted with PBS for immunosensor tests and each experiment was repeated for four times. The recoveries from detections results were calculated as the averages of four replicates and shown in Table S1, giving the range 90.36 %–106.40 % (corn flour) and 87.65 %–109.04 % (corn based baby food) with all RSDs less than 10 %. The above results suggested that this immunosensor assay was feasible for detecting ZEN reliably in real corn based products with simple pretreatment.

Conclusion

In summary, a sensitive and cost-effective label-free immunosensor was constructed based on the oriented immobilization of a MAb specific for ZENs and DPV intensity as the readout signal for direct detection of family ZENs. The applications of MWCNTs and AuPt-NPs enhanced the conductibility and provided large surface area for loading biomolecules. MAb was immobilized efficiently towards SPA which increased the sensitivity of the immunosensor. With excellent sensitivity, high reproducibility and stability, good selectivity and satisfactory accuracy for ZENs, the immunosensor, coupled with simple pretreatment, provide a feasible and reliable way for monitoring family ZENs in real food samples.

Acknowledgments This work was supported by the "973" program (2013CB127801), Shanghai Municipal Commission for Science and Technology (15230724400 and 14391901800), and the Public Science and Technology Research Funds of State Grains Bureau (201313005-01-2 and 201513006-02).

Compliance with ethical standards The authors declare that they have no competing interests.

References

1. Shier WT, Shier AC, Xie W, Mirocha CJ (2001) Structure-activity relationships for human estrogenic activity in zearalenone mycotoxins. Toxicon 39:1435–1438
2. Kakeya H, Takahashi-Ando N, Kimura M, Onose R, Yamaguchi I, Osada H (2002) Biotransformation of the mycotoxin, zearalenone, to a non-estrogenic compound by a fungal strain of Clonostachys sp. Biosci Biotechnol Biochem 66:2723–2726
3. Juan C, Ritieni A, Mañes J (2012) Determination of trichothecenes and zearalenones in grain cereal, flour and bread by liquid chromatography tandem mass spectrometry. Food Chem 134:2389–2397
4. Busk Ø, Ndossi D, Frizzell C, Verhaegen S, Uhlig S, Eriksen G, Connolly L, Ropstad E, Sørlie M (2012) Changes in the proteome

of the H295R steroidogenesis model associated with exposure to the mycotoxin zearalenone and its metabolites, α- and β-zearalenol. In: Rodrigues P, Eckersall D, de Almeida A (eds) Farm animal proteomics. Wageningen, Netherlands, pp. 55–58
5. Aldana JR, Silva LJ, Pena A, Mañes J, Lino CM (2014) Occurrence and risk assessment of zearalenone in flours from Portuguese and Dutch markets. Food Control 45:51–55
6. Qian M, Zhang H, Wu L, Jin N, Wang J, Jiang K (2015) Simultaneous determination of zearalenone and its derivatives in edible vegetable oil by gel permeation chromatography and gas chromatography–triple quadrupole mass spectrometry. Food Chem 166:23–28
7. Hsieh HY, Shyu CL, Liao CW, Lee RJ, Lee MR, Vickroy TW, Chou CC (2012) Liquid chromatography incorporating ultraviolet and electrochemical analyses for dual detection of zeranol and zearalenone metabolites in mouldy grains. J Sci Food Agric 92:1230–1237
8. Huang H, Tan Y, Shi J, Liang G, Zhu JJ (2010) DNA aptasensor for the detection of ATP based on quantum dots electrochemiluminescence. Nanoscale 2:606–612
9. Monerris MJ, Arévalo FJ, Fernández H, Zon MA, Molina PG (2015) Development of a very sensitive electrochemical immunosensor for the determination of 17β-estradiol in bovine serum samples. Sens Actuator B Chem 208:525–531
10. Tang D, Su B, Tang J, Ren J, Chen G (2010) Nanoparticle-based sandwich electrochemical immunoassay for carbohydrate antigen 125 with signal enhancement using enzyme-coated nanometer-sized enzyme-doped silica beads. Anal Chem 82:1527–1534
11. Loyprasert S, Thavarungkul P, Asawatreratanakul P, Wongkittisuksa B, Limsakul C, Kanatharana P (2008) Label-free capacitive immunosensor for microcystin-LR using self-assembled thiourea monolayer incorporated with Ag nanoparticles on gold electrode. Biosens Bioelectron 24:78–86
12. Thavarungkul P, Dawan S, Kanatharana P, Asawatreratanakul P (2007) Detecting penicillin G in milk with impedimetric label-free immunosensor. Biosens Bioelectron 23:688–694
13. Dai S, Wu S, Duan N, Wang Z (2016) A luminescence resonance energy transfer based aptasensor for the mycotoxin ochratoxin a using upconversion nanoparticles and gold nanorods. Microchim Acta 183:1909–1916
14. Moreno V, Zougagh M, Ríos Á (2016) Hybrid nanoparticles based on magnetic multiwalled carbon nanotube-nanoC18SiO2 composites for solid phase extraction of mycotoxins prior to their determination by LC-MS. Microchim Acta 183:871–880
15. Viswanathan S, Rani C, Anand AV, Ho JA (2009) Disposable electrochemical immunosensor for carcinoembryonic antigen using ferrocene liposomes and MWCNT screen-printed electrode. Biosens Bioelectron 24:1984–1989
16. Kavosi B, Salimi A, Hallaj R, Amani K (2014) A highly sensitive prostate-specific antigen immunosensor based on gold nanoparticles/PAMAM dendrimer loaded on MWCNTS/chitosan/ionic liquid nanocomposite. Biosens Bioelectron 52:20–28
17. Banks CE, Compton RG (2006) New electrodes for old: from carbon nanotubes to edge plane pyrolytic graphite. Analyst 131:15–21
18. Popov VN (2004) Carbon nanotubes: properties and application. Mater Sci Eng R 43:61–102
19. Chen Y, Cao H, Shi W, Liu H, Huang Y (2013) Fe–Co bimetallic alloy nanoparticles as a highly active peroxidase mimetic and its application in biosensing. Chem Commun 49:5013–5015
20. Chen KJ, Lee CF, Rick J, Wang SH, Liu CC, Hwang BJ (2012) Fabrication and application of amperometric glucose biosensor based on a novel PtPd bimetallic nanoparticle decorated multi-walled carbon nanotube catalyst. Biosens Bioelectron 33:75–81
21. Safavi A, Farjami F (2011) Electrodeposition of gold–platinum alloy nanoparticles on ionic liquid–chitosan composite film and its application in fabricating an amperometric cholesterol biosensor. Biosens Bioelectron 26:2547–2552
22. Feng R, Zhang Y, Li H, Wu D, Xin X, Zhang S, Yu H, Wei Q, Du B (2013) Ultrasensitive electrochemical immunosensor for zeranol detection based on signal amplification strategy of nanoporous gold films and nano-montmorillonite as labels. Anal Chim Acta 758:72–79
23. Liu L, Chao Y, Cao W, Wang Y, Luo C, Pang X, Fan D, Wei Q (2014) A label-free amperometric immunosensor for detection of zearalenone based on trimetallic Au-core/AgPt-shell nanorattles and mesoporous carbon. Anal Chim Acta 847:29–36
24. Xue X, Wei D, Feng R, Wang H, Wei Q, Du B (2013) Label-free electrochemical immunosensors for the detection of zeranol using graphene sheets and nickel hexacyanoferrate nanocomposites. Anal Methods 5:4159–4164
25. Regiart M, Seia MA, Messina GA, Bertolino FA, Raba J (2015) Electrochemical immunosensing using a nanostructured functional platform for determination of α-zearalanol. Microchim Acta 182:531–538
26. Regiart M, Pereira SV, Spotorno VG, Bertolino FA, Raba J (2014) Food safety control of zeranol through voltammetric immunosensing on Au–Pt bimetallic nanoparticle surfaces. Analyst 139:4702–4709
27. Tang DQ, Zhang DJ, Tang DY, Ai H (2006) Amplification of the antigen–antibody interaction from quartz crystal microbalance immunosensors via back-filling immobilization of nanogold on biorecognition surface. J Immunol Methods 316:144–152
28. Oh BK, Kim YK, Park KW, Lee WH, Choi JW (2004) Surface plasmon resonance immunosensor for the detection of salmonella typhimurium. Biosens Bioelectron 19:1497–1504
29. Oh BK, Chun BS, Park KW, Lee W, Lee WH, Choi JW (2004) Fabrication of protein G LB film for immunoglobulin G immobilization. Mat Sci Eng C Mater 24:65–69
30. Makaraviciute A, Ramanaviciene A (2013) Site-directed antibody immobilization techniques for immunosensors. Biosens Bioelectron 50:460–471
31. Trilling AK, Beekwilder J, Zuilhof H (2013) Antibody orientation on biosensor surfaces: a minireview. Analyst 138:1619–1627
32. Anderson GP, Jacoby MA, Ligler FS, King KD (1997) Effectiveness of protein a for antibody immobilization for a fiber optic biosensor. Biosens Bioelectron 12:329–336
33. Liu Y, Yu J (2016) Oriented immobilization of proteins on solid supports for use in biosensors and biochips: a review. Microchim Acta 183:1–19
34. Lee W, Oh BK, Bae YM, Paek SH, Lee WH, Choi JW (2003) Fabrication of self-assembled protein a monolayer and its application as an immunosensor. Biosens Bioelectron 19:185–192
35. Liu G, Han Z, Nie D, Yang J, Zhao Z, Zhang J, Li H, Liao Y, Song S, De Saeger S, Wu AB (2012) Rapid and sensitive quantitation of zearalenone in food and feed by lateral flow immunoassay. Food Control 27:200–205
36. Arribas AS, Bermejo E, Chicharro M, Zapardiel A, Luque GL, Ferreyra NF, Rivas GA (2007) Analytical applications of glassy carbon electrodes modified with multi-wall carbon nanotubes dispersed in polyethylenimine as detectors in flow systems. Anal Chim Acta 596:183–194
37. Upadhyay S, Rao GR, Sharma MK, Bhattacharya BK, Rao VK, Vijayaraghavan R (2009) Immobilization of acetylcholineesterase–choline oxidase on a gold–platinum bimetallic nanoparticles modified glassy carbon electrode for the sensitive detection of organophosphate pesticides, carbamates and nerve agents. Biosens Bioelectron 25:832–838
38. Tao M, Li X, Wu Z, Wang M, Hua M, Yang Y (2011) The preparation of label-free electrochemical immunosensor based on the Pt–Au alloy nanotube array for detection of human chorionic gonadotrophin. Clin Chim Acta 412:550–555
39. Sun X, Zhu Y, Wang X (2012) Amperometric immunosensor based on deposited gold nanocrystals/4, 4′-thiobisbenzenethiol for determination of carbofuran. Food Control 28:184–191